Remote Sensing Detection of Wheat Stripe Rust by Synergized Solar-Induced Chlorophyll Fluorescence and Differential Spectral Index

Xia Jing
Xi'an University of Science and Technology,
College of Geometrics,
Xi'an, China
e-mail: jingxiaxust@163.com

Zongfan Bai
Xi'an University of Science and Technology,
College of Geometrics,
Xi'an, China
e-mail: bzf1529@163.com

Abstract—Remote sensing detection of wheat stripe rust is important for agriculture management. In order to improve detection accuracy of the disease severity of wheat stripe rust, a detection method based on solar-induced chlorophyll fluorescence combined with differential spectral index was proposed in the paper. This method makes full use of the advantages of reflectance spectroscopy in detecting biochemical parameters and the advantages of chlorophyll fluorescence in photosynthetic physiology diagnosis. A characteristic dataset was collected from 13 differential spectral indices sensitive to the severity of wheat stripe rust, and different chlorophyll fluorescence values extracted by measuring radiance or reflectance respectively. The dataset was then processed using two different methods—partial least squares(PLS),and BP neural network—to carry out the remote sensing detection of wheat stripe rust severity. The results showed that: (1) The models based on the solar-induced chlorophyll fluorescence combined with spectral indices are more accurate than those based on differential spectral index. (2) The disease severity prediction model of wheat stripe rust constructed by BP neural network is better than PLS approaches. The research results of this paper have important significance for improving the accuracy of remote sensing detection of wheat stripe rust severity, and provide new information and a theoretical framework for remote sensing detection of other crop diseases.

Keywords: Solar-induced Chlorophyll Fluorescence; Wheat Stripe Rust; Differential Spectral Index; Synergy

I. INTRODUCTION

Wheat stripe rust is a disease found across a wide area of China that causes a significant amount of damage to wheat production[1]. Once it breaks out, the yield and quality of wheat will be seriously affected if the disease cannot be promptly detected, reported, and contained. Since remote sensing technology has the advantage of gathering rapid, wide-area observations and measurements without damaging crops, the use of remote sensing data to detect wheat stripe rust has become a research topic of significant interest amongst scientists, and significant progress has been made in this field[2-8]. The current research focuses on the use of reflectance spectroscopy to detect wheat stripe rust disease information, and it attempts to identify reflectance spectral bands[5,6] and spectral differential indices[7,8] that are sensitive to wheat stripe rust. The reflectance spectrum mainly provides information about the dynamics of plant biophysical properties such as photosynthesis, leaf water content, leaf area index, and chlorophyll content[9]. It does not directly reveal the photosynthetic physiological state of the vegetation[10,11]. Compared to reflectance spectroscopy, chlorophyll fluorescence (ChlF) measurements contain more direct information about physical states related to the physiological functioning of vegetation[12]. This metric is used as a "probe" to evaluate the health status of plants because it can quickly and sensitively provide information about the physiological state of the plants without damaging them, as well as information regarding the relationship between the plants and the wider environment[13]. Some studies have found that the chlorophyll fluorescence spectrum can reflect the physiological changes caused by the disease in question earlier and with more sensitivity than the reflectance spectrum can[14,15]. By detecting the spectral characteristics of fluorescence, the physiology, growth, disease severity, and stress state of plants can be more rapidly and accurately understood[15,16].

At present, there are few studies evaluating the monitoring of crop diseases by measuring SIF. Zhang Yongjiang et al. used the standard Fraunhofer Line Discrimination (FLD) method to estimate the solar-induced chlorophyll fluorescence of different levels of wheat stripe rust severity. Their research demonstrated that SIF information can detect and measure incidences of wheat stripe rust in fields[17]. Similarly, Raji et al. monitored cassava mosaic disease by extracting SIF information from solar reflectance spectra based on the Fraunhofer line theory. Their results showed that SIF has good potential for plant disease monitoring[14]. It is notable that the data sources used in the above studies were mainly single reflectance spectroscopy datasets or solar-induced chlorophyll fluorescence datasets, so they did not combine the advantages of reflectance spectroscopy in detecting biochemical parameters and the advantages of using chlorophyll fluorescence for photosynthetic physiological diagnosis when using remote sensing for the evaluation of crop condition. To this end, this paper will combine SIF and reflectance spectroscopy to establish an improved method for the remote sensing detection of the severity of wheat stripe rust.

In order to detect the severity of wheat stripe rust by remote sensing, it is necessary to select an appropriate method to establish the wheat stripe rust severity estimation model. At present, the modeling method used to monitor the severity of wheat stripe rust is mainly based on a regression analysis method[18,19], which is simple to calculate and easy to implement. Due to typical variations in external conditions during data acquisition, however, the mathematical statistical models established based on regression analysis have poor universality[20]. Many scholars have, therefore, applied machine learning

978-1-7281-5712-2/19/$31.00 ©2019 IEEE
DOI 10.1109/ICISCE48695.2019.00224

algorithms to remote sensing data to standardize the detection of the severity of wheat stripe rust, and have achieved good results. Lihong Mo, for example, constructed an inversion model that estimated the number of wheat stripe rust bacteria using a neural network algorithm[21]. Hu Xiaoping et al. made a short-term prediction of the prevalence of wheat stripe rust in Hanzhong based on a back propagation (BP) neural network[22]. Although machine learning algorithms have achieved significant results when estimating wheat stripe rust, machine learning algorithms have not yet been used with combined radiance fluorescence, reflectance fluorescence, and differential spectral indices for remote sensing evaluations of wheat stripe rust.

In this study, we first used radiance and reflectance fluorescence indices to estimate the solar-induced chlorophyll fluorescence intensity of crops experiencing different levels of severity of wheat stripe rust. Second, we constructed severity estimation models of wheat stripe rust by using BP neural network, and partial least squares (PLS) algorithms. Third, we carried out remote sensing detection estimations of disease severity for wheat stripe rust on crops using SIF and reflectivity spectra. Finally, we also compared and analyzed the accuracy of the estimates of disease severity of wheat stripe rust in crops using different data sources and modeling methods, and with respect to a cross-validation method. As a result, we were able to determine the most appropriate model and method for the remote sensing detection and estimation of disease severity of wheat stripe rust in crops. The results have important significance for improving the accuracy of the remote sensing detection and estimation of wheat stripe rust levels, and the study provides new information for the successful implementation of the wide-area remote sensing monitoring of crop health.

II. MATERIALS AND METHODS

A. Experimental design

The geographical area covered in this experiment is located around the Experimental Station of the Chinese Academy of Agricultural Sciences in Langfang City, Hebei Province (39°30'40"N, 116°36'20"E). The wheat variety grown in the study area is "Mingxian No. 169", which is sensitive to stripe rust. The average wheat planting density in the test area was 113 stalks/m^2. On April 9, 2018, the wheat was subjected to strip rust fungal infection by a spray method using a spore solution having a concentration of 9 mg/100 ml. The wheat in the experimental area was divided into a healthy group (in two areas designated A and D) and an infected group (in two areas designated B and C). The area covered by each experimental group was 220 m2. Each area comprised 8 squares (A3-A10, B1-B8, C1-C8, and D1-D8), so that there were 16 sample squares for the healthy group and 16 for the infected group.

B. Disease index survey and field canopy spectral measurement

1) Canopy spectral measurement

In this experiment, canopy spectral data of crops with wheat stripe rust of different severity levels were measured on May 14, May 18, and May 24, 2018. The instrument used for the measurement were ASD Field Spec 4 and QE pro spectrometers. The measuring height was 1.3 m above the ground and the probe field angle was 25°. Each area was measured 10 times repeatedly and corrected with a standard BaSO4 reference plate before and after each measurement. The reflectance value was then calculated according to formula (1):

$$R = \frac{L_{target}}{L_{board}} \times R_{board} \qquad (1)$$

where R is the canopy reflectivity, L_{target} is the target radiance, L_{board} is the reference plate radiance, and R_{board} is the reference plate reflectivity.

2) Disease index survey

Investigation of the canopy disease index was carried out using the 5-point sampling method. Five points of symmetry were selected in each plot, covering about 1 m^2 per point, and 30 wheat plants were randomly selected to investigate the disease incidence levels. The severity of the disease was quantified by referring to the national standard "Technical Specification for Wheat Stripe Rust" (GB/T15795)[23]. The single leaf disease severity was classified according to 9 gradients, so that the leaf lesion coverage was estimated as 0%, 1%, 10%, 20%, 30%, 45%, 60%, 80%, and 100%. The number of wheat leaves with each level of severity was recorded, and the disease index for different gradient test groups was calculated using the following equation [24]:

$$DI = \frac{\Sigma\ (x \times f)}{n \times \Sigma f} \qquad (2)$$

where DI is the disease index, x is the gradient value, n is the highest gradient grade, and f is the number of leaves for each gradient.

3) Extraction of solar-induced chlorophyll fluorescence

The extraction algorithm for estimating solar-induced chlorophyll fluorescence mostly includes radiance and reflectivity[25]. The radiance-based solar-induced chlorophyll fluorescence extraction algorithm uses the Fraunhofer line principle. The apparent radiance of a band within the Fraunhofer line and one (or more) bands outside the Fraunhofer line are used to calculate the intensity of the chlorophyll fluorescence by calculating the degree of filling of the "Fraunhofer well" by fluorescence excited by sunlight under natural light conditions [25]. The radiance-based chlorophyll fluorescence extraction algorithm provides a direct estimate of the fluorescence intensity value. The reflectance-based chlorophyll fluorescence extraction algorithm produces fluorescence information by analyzing the influence of fluorescence on the reflectivity of the red edge region. A reflectance index is obtained which estimates the fluorescence intensity, instead of estimating an independent physical quantity, so it can be regarded as a kind of indirect chlorophyll fluorescence extraction and estimation algorithm[26].

a. Radiation method

The simplest method for extracting sunlight-induced chlorophyll fluorescence values using radiance is the standard Fraunhofer Line discrimination algorithm. This

method assumes that the reflectance and transmittance inside and outside the absorption line are equal. The chlorophyll fluorescence intensity F[27] at the Fraunhofer line was calculated by comparing the spectral differences between the upstream radiance and the downstream irradiance of the canopy, for the two bands in the inner and outer bands of the Fraunhofer line.

$$F = \frac{L_{in} \times I_{out} - L_{out} \times I_{in}}{I_{out} - I_{in}} \quad (3)$$

In the formula, I_{in} and I_{out} are the spectral intensities of the solar irradiance inside and outside the Fraunhofer line; and L_{in} and L_{out} are the radiance intensities of the vegetation canopy reflection inside and outside the Fraunhofer line.

Although the standard FLD algorithm is simple to operate, the reflectance and fluorescence values of the inner and outer bands of the absorption line are often different, which affects the accuracy of the fluorescence estimates[24]. To overcome the limitations of the standard FLD method hypothesis, Maier et al.[28] proposed an improved 3FLD fluorescence estimation algorithm. The algorithm considers that the chlorophyll fluorescence and reflectance spectra are linearly varying around the absorption line band[29]. It uses the weighted average of the left and right bands of the absorption line to replace the single band value in the standard FLD algorithm. The error caused by the assumption of constant fluorescence and reflectance in the standard FLD method is, therefore, reduced to some extent, and the estimation accuracy of SIF is improved. Liu et al. also showed that the 3FLD method is the most robust algorithm for SIF detection[30]. Based on this, the 3FLD method is used to calculate the SIF. The calculation formula is shown in equations (4), (5), and (6):

$$I_{out} = \omega_{left} \times I_{left} + \omega_{right} \times I_{right} \quad (4)$$

$$L_{out} = \omega_{left} \times L_{left} + \omega_{right} \times L_{right} \quad (5)$$

In this formula, $\omega_{\text{left}} = \frac{\lambda_{\text{right}} - \lambda_{in}}{\lambda_{right} - \lambda_{left}}$, $\omega_{\text{right}} = \frac{\lambda_{\text{in}} - \lambda_{left}}{\lambda_{right} - \lambda_{left}}$, and $\lambda_{\text{in}}, \lambda_{\text{left}}, \lambda_{\text{right}}$ are the wavelengths within the absorption line, and the wavelengths of the left and right bands of the absorption line, respectively. ω_{left} and ω_{right} are the weights of the two reference bands on the left and right of the absorption line. I_{left} and I_{right} are the spectral intensities of the solar irradiance of the left and right lines of the absorption line respectively, and L_{left} and L_{right} are the spectral intensities of the canopy reflection radiance of the vegetation line around the absorption line, respectively.

Bringing equations (4) and (5) into equation (3), the chlorophyll fluorescence intensity in the absorption line can be obtained, as shown in (6):

$$\overline{F_{in}} = \frac{L_{in} \times (\omega_{left} \times I_{left} + \omega_{right} \times I_{right}) - I_{in} \times (\omega_{left} \times L_{left} + \omega_{right} \times L_{right})}{(\omega_{left} \times I_{left} + \omega_{right} \times I_{right}) - I_{in}} \quad (6)$$

To reduce the influence of external factors such as variations in solar light intensity at different time periods on the estimates of solar-induced chlorophyll fluorescence during canopy spectral data measurement, and to improve the accuracy of the solar-induced chlorophyll fluorescence estimates, the absolute intensity ($W/m^2/nm/sr$) of the calculated solar-induced chlorophyll fluorescence was divided by the solar incident irradiance in the Fraunhofer absorption line, and the relative intensity of solar-induced chlorophyll fluorescence at the absorption line was obtained.

b. Reflectivity method

The algorithm for calculating the chlorophyll fluorescence index under natural light conditions uses the reflectance index to estimate the intensity of the fluorescence. The algorithm calculates the influence of the fluorescence on the reflectance of the red edge region. Typically, the solar-induced chlorophyll fluorescence index based on the reflectance index incorporates a reflectance ratio, a derivative, and an infilling index[24]. The reflectivity ratio index is obtained by comparing the reflectivity band strongly affected by fluorescence with a band weakly affected by fluorescence. The procedure removes spectral information related to reflectivity and obtains fluorescence information by calculating the ratio between the two values. The infilling index represents fluorescence information indirectly by evaluating the difference between the reflectance values for the two bands, but the index is also affected by the depth of the Fraunhofer line and the magnitude of the fluorescence. Since changes in the geometry of the atmosphere and the sun will affect the depth of the Fraunhofer line, the index is only applicable to data comparisons made at the same time of day and year and under the same observation conditions[24].This paper, therefore, mainly uses the reflectance ratio and the derivative of reflectivity to calculate the solar-induced chlorophyll fluorescence under severe wheat stripe rust conditions.

4) Hyperspectral differential index

Differential processing of the reflectance spectrum can enhance the subtle changes in the slope of the spectral curve removing the effects of linear or near-linear background spectrum noise on the target spectrum[31]. In this paper, we combined the results from existing research relating to the use of a hyperspectral differential index to monitor wheat stripe rust[32], and calculated the differential spectral index as shown in Table 1.

TABLE I. LIST OF DIFFERENTIAL SPECTRAL INDICES

Feature parameter	Definition
SDg	First-order differential sum in the green edge (501-560nm) (501-560nm)
SDb	First-order differential sum in the blue edge (430-500nm)
SDr	First-order differential sum in the red edge (680-760nm)
Dr	First-order differential maximum in the red edge range
Dg	First-order differential maximum in the green edge range
D725	First order differential value at 725 nm
D750	First order differential value at 750 nm

Due to the discreteness of the spectral sampling interval, the first-order differential spectroscopy is generally approximated by a differential method [33]:

$$\rho'(\lambda_i) = [\rho(\lambda_{i+1}) - \rho(\lambda_{i-1})] / 2\Delta\lambda \quad , (7)$$

where λ_i is the wavelength of each band, $\rho'(\lambda_i)$ is the first-order differential spectrum, and $\Delta\lambda$ is the interval of wavelength λ_{i+1} to λ_{i-1}.

C. Model Construction Method

In order to determine the most appropriate model to use for generating remote-sensing based estimates of wheat stripe rust, this paper uses the partial least squares regression analysis based on mathematical statistics, a BP neural network algorithm based on machine learning to construct models for estimating wheat stripe rust severity. Verification methods were used to analyze and evaluate the accuracy of each model.

1) Partial least squares regression analysis

PLS is a principal component regression statistical method that finds the best matching function for representing a dataset by minimizing the sum of squared errors. In the modeling process, the algorithm uses principal component analysis to judge whether independent variables added to the modeling can significantly improve the estimation ability and avoid collinear variables that may appear in the PLS regression. The method can, therefore, interpret multiple correlations between multiple hyperspectral features and construct regression models using all valid data[33].

2) BP neural network model

In neural network models, BP is a widely used technique. The topology of the BP neural network model includes an input layer, a hidden layer, and an output layer. The neurons between the layers are connected by a full interconnection, and are connected to each other by corresponding network weight coefficients, while the neurons in each layer are not connected. The core idea is to adjust the weight between each neuron, while the error is reversed from the hidden layer to the input layer, layer by layer, and the error function is a “chain derivation” used to make the error close to the minimum [20].

III. RESULT

A. Optimization of remote sensing detection factors for wheat stripe rust

1) Chlorophyll fluorescence estimation and screening of sensitive factors

The Fraunhofer formed by two oxygen absorption bands at the O2-B (688nm) and O2-A (760nm) frequencies have obvious characteristics, and the fluorescence is strong[35]. In this study, the 688nm and 760nm bands were used to calculate the chlorophyll fluorescence intensity of the vegetation canopy. First, the absolute intensity of the solar-induced chlorophyll fluorescence based on 3FLD algorithm at the Fraunhofer, formed by the two oxygen absorptions at 688 nm and 760 nm, respectively ($W/m^2/nm/sr$). Then, in order to reduce the influence of external conditions such as solar illumination during the measurement of canopy spectral data, and to improve the accuracy of the estimated chlorophyll fluorescence due to photosynthesis, the absolute intensity of the chlorophyll fluorescence was divided by the incident irradiance in the Fraunhofer absorption line, to obtain the relative intensities of photosynthesis chlorophyll fluorescence at the two oxygen absorption lines at 760 nm and 688 nm. On the basis of this, the relationship between the severity of wheat stripe rust and the relative intensity of the chlorophyll fluorescence was established (Table 2).

The red edge region of the vegetation spectrum (650~800nm) contains information about the molecular structure of plant cells and is commonly used to evaluate plant health. Chlorophyll fluorescence is also found in the red edge region, and contributes to the apparent reflectivity of this region, so that many fluorescence spectral indices can be constructed[31]. These include R_{685}/R_{655}, R_{690}/R_{655}, R_{740}/R_{720}, R_{440}/R_{690}, and R_{750}/R_{800} as developed by Zarco-Tejada[36,37], and R_{740}/R_{800}[38] as proposed by Dobrowski. Zarco-Tejada et al.[39] developed the first derivative spectral index D_{705}/D_{722}, D_{730}/D_{706}. The ratio function in these indices can remove the effect of spectral information related to reflectivity, so that small changes of the fluorescence emissions in the red edge spectral region can be detected, and chlorophyll fluorescence information can be obtained. The abovementioned reflectance fluorescence spectral index was calculated based on this, and correlated with the severity of wheat stripe rust (Table 2) to identify the remote sensing detection

factors which are sensitive to the severity of wheat stripe rust disease.

TABLE 2 RELATION BETWEEN DI AND SIF (n=52, The extremely significant level is 0.354 same as below)

SIF	Complex correlation coefficient	SIF	Complex correlation coefficient
3FLD-760nm	-0.6722**	R_{740}/R_{720}	-0.6194**
3FLD-688nm	-0.4924**	R_{440}/R_{690}	-0.7187**
R_{685}/R_{655}	+0.3063*	R_{750}/R_{800}	+0.0036
R_{690}/R_{655}	-0.0868	D_{705}/D_{722}	+0.7104**
R_{740}/R_{800}	+0.4539**	D_{730}/D_{706}	-0.6831**

Note: ** represents the strongly significant level of 1%, * represents the significant level of 5%, the same below

It can be seen that, of the ten SIF cases presented in Table 2, seven are significantly correlated with the severity of wheat stripe rust. These are the three reflectance fluorescence indices R_{740}/R_{800}, R_{740}/R_{720}, R_{440}/R_{690}, plus the two derivative fluorescence indices D_{705}/D_{722}, D_{730}/D_{706}, and the two estimated relative intensities of chlorophyll fluorescence, based on the radiance method, at the O2-A absorption line and the O2-B absorption line. These are all significantly correlated with the severity of wheat stripe rust and can, therefore, be used as chlorophyll fluorescence parameters representative of wheat stripe rust when detected by remote sensing. It should be noted that the relative intensities of chlorophyll fluorescence at the O2-A absorption line and the O2-B absorption line were significantly negatively correlated with the severity of wheat stripe rust. This is because, as the severity of wheat stripe rust increases, the chlorophyll content decreases rapidly, so photosynthesic activity decreases, and absorbed photosynthetic active radiation (APARchl) is reduced[40]. Similarly, SIF is mainly driven by APARchl[41], therefore, the SIF signal also decreases with the decrease of APARchl, and there is a significant negative correlation between SIF and DI.

2) Differential spectral index optimization

In order to identify the differential spectral indices sensitive to the severity of wheat stripe rust, this study used formula (2) to first differentiate the canopy spectral data under different severities of wheat stripe rust, and then obtain the differential spectral index of each band. These indices were correlated with the severity of wheat stripe rust (Table 3).

It can be seen from Table 3 that the correlation between SDg and Dg and the severity of wheat stripe rust is not significant, but the remaining 11 differential spectral indices in Table 3 are significantly correlated with the severity of wheat stripe rust, and can be used as independent variables to incorporate into estimates of the severity of wheat stripe rust

TABLE 3 RELATION BETWEEN DI AND DIFFERENTIAL SPECTRAL (n=52)

Feature	Complex correlation coefficient	Feature	Complex correlation coefficient
Dg	0.1018	SDr/SDg	-0.5863**
Dr	-0.5473**	SDg/SDb	-0.7391**
SDb	+0.6669**	(SDr-SDb)/(SDr+SDb)	-0.6229**
SDg	+0.0201	(SDr-SDg)/(SDr+SDg)	-0.5887**
SDr	-0.4562**	(SDg-SDb)/(SDg+SDb)	-0.6890**
SDr/SDb	-0.8122**	D750	-0.6055**
		D725	-0.5494**

B. Model Construction and Accuracy Analysis

In order to verify the reliability and stability of the models and evaluate the results produced, the study incorporated a cross-checking method based on measurements of control samples. Fifty-two raw crop samples (47 infected samples, 5 healthy samples) were randomly divided into two parts, the first part including 39 datasets (35 infected samples and 4 healthy samples) was used as the training set for the model, and the remaining 13 data samples (12 infected samples and 1 healthy sample) were used as validation sample group used to evaluate the accuracy of the models. In the study, the validation data were used to establish the models estimating wheat stripe rust severity. The coefficient of determination (R^2) and root mean square error (RMSE) were then used as parameters for evaluating the effectiveness of the models. Their accuracy at estimating the severity of wheat stripe rust, based on the different data sources and different algorithms, was then compared and analyzed.

1) Construction of the PLS estimation model

When using the partial least squares algorithm to construct the model for estimating the severity of wheat stripe rust, the cross-validity analysis was first used to

determine the optimal number of components for the PLS algorithm. In this experiment, when the independent variable of the model was the differential spectral index, the optimal number of principal components was two. If the chlorophyll fluorescence synergistic differential spectral index was used as an independent variable, the optimal number of principal components was three. The estimated results are shown in Figure 1. Figure 1(a) shows the model's estimated results when using the differential spectral index as an independent variable. Figure 1(b) shows the model's estimated results when using a fusion of the differential spectral index and the SIF as independent variables. In the figure, the abscissa is the measured severity of wheat stripe rust, and the ordinate is the severity of the wheat stripe rust estimated by the model. The solid line is a 1:1 relationship line.

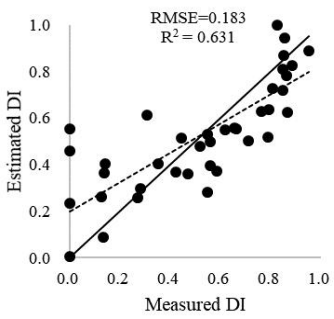

a.differential spectral index as independent variable

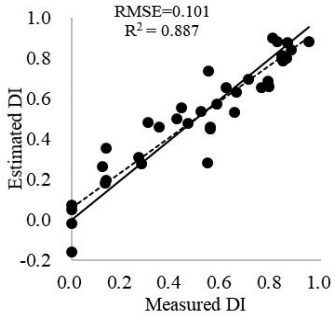

b.SIF and differential spectral index as independent variable

Figure. 1 PLS stripe model predictions of wheat stripe rust severity (n=39; the significant level of pronounced significance was 0.408, the same as below)

Figure 1(a) show the R^2 for models estimating the DI and the measured DI of the wheat stripe rust severity using the PLS algorithm. The algorithm in Figure 1(b) combines the solar-induced chlorophyll fluorescence and the differential spectral index as independent variables, and the resultant values is 0.887. This value are higher than the values for the models in Figure 1(a) only used the differential spectra were independent variables. The RMSEs for the models shown in Figure 1(b) is 0.101, which were lower than the RMSEs for only differential spectra as the independent variable, as shown in Figure 1(a). The accuracy of the PLS model using the chlorophyll fluorescence and differential spectral index as the independent variables was, therefore, higher than that for the differential spectral index alone.

2) Construction of the BP neural network estimation model

The BP neural network model in this study consisted of a standard three-layer network structure including an input layer (sensitive to wheat stripe rust), a hidden layer, and an output layer (representing the severity of wheat stripe rust). The hidden layer is setup as 5 nerves, the input layer to the hidden layer transfer function is logsig, and the hidden layer to the output layer transfer function is purelin. The specific parameter settings are shown in Table 4. In order to obtain a better network training effect, each input variable was normalized before modeling.

The reflectivity differential spectral index, the synergistic differential spectral index, and the solar-induced chlorophyll fluorescence were used as independent variables, and the severity of the wheat stripe rust disease was used as a dependent variable to construct the BP neural network model for estimating wheat stripe rust severity. The model construction results are shown in figure 2.

Figure 2(a) and (b) show the determination coefficients for models of estimated and measured DI of the wheat stripe rust severity using the BP neural network algorithm. Figure2(b) combines the solar-induced chlorophyll fluorescence and the differential spectral index as independent variables, and the resultant value is 0.861. This values is higher than the model determination coefficients using only the differential spectra as independent variables. Similarly, the RMSE for the models shown in Figure 2(a) were 0.112, which were lower values than the RMSE using only differential spectra as the independent variables in the model. The accuracy of the BP neural network model with the chlorophyll fluorescence and differential spectral indices as the independent variables was, therefore, higher than that for the model using only the differential spectral indices.

TABLE 4 PARAMETER VALUES FOR THE BP NEURAL NETWORK ALGORITHM

Parameter	Value	Parameter	Value
Maximum number of training	5000	Training interval	10
Minimum mean square error	0.001	Learning step	0.1

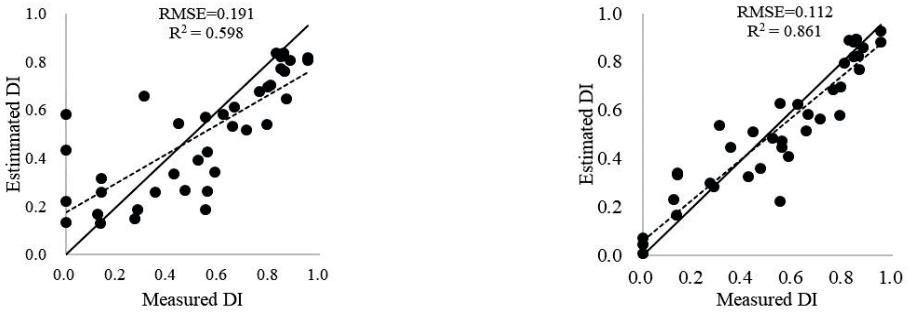

a.differential spectral index as independent variable b.SIF and differential spectral index as independent variable

Figure. 2 Prediction of the severity of wheat stripe rust by BP neural network model (n=39)

3) Model accuracy evaluation

In this paper, the test group data were used to test the wheat stripe rust disease severity estimation model constructed by two algorithms, and the results were shown in figure 3. The figures show the R^2 and RMSE of the test results using different data sources and different algorithms.

It was clear that all two algorithm models had good estimation accuracy but the accuracy of the estimates made using the BP neural network models were higher than those made by the PLS models. Using the BP neural network model with the verification data sets, and using the combination of solar-induced chlorophyll fluorescence and differential spectral index values as independent variables, the R^2 between the estimated DI and the measured DI values is 0.955. This value is higher than the R^2 based on the PLS model (0.916). Similarly, the RMSE values using the combined independent variables and the BP neural network model was 0.068. This value was smaller than the RMSE using the PLS model (0.094). When compared with PLS models then, the remote sensing models for estimating wheat stripe rust based on the BP neural network algorithm had a higher estimation accuracy and generalization ability, and so this approach is a more suitable choice for carrying out remote sensing detection of wheat stripe rust severity in real world applications.

Comparison and analysis of the results based on using the differential spectral indices as independent variables shows that they are not as good as the results based on using the fusion of SIF and differential spectral indices as independent variables. In conclusion, the study demonstrated the most effective approach to use to ensure comprehensive utilization of canopy spectral data to provide crop growth information and to identify the chlorophyll fluorescence parameters that reflect the vitality of crop photosynthesis. These approaches can be used to significantly improve the accuracy of wheat stripe rust estimates using remote sensing systems.

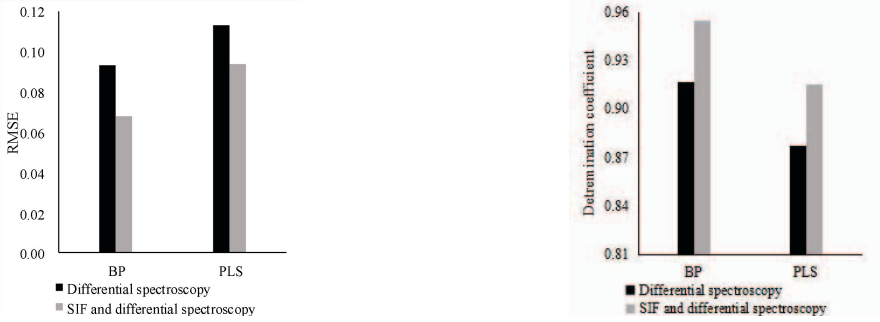

a.Coefficients of determination of predictive model test sets b.RMSE of predictive model test sets

Figure.7 predictive model test results

IV. DISCUSSION

In this paper, data measuring the intensity of chlorophyll fluorescence were extracted using radiance and reflectance. The relative intensities of chlorophyll fluorescence extracted by the radiance method were both strongly significantly correlated with the severity of the wheat stripe rust, while the correlation between the relative intensity of chlorophyll fluorescence for the O2-A band and the severity of wheat stripe rust was higher than the correlation for the O2-B band. The reflectance fluorescence indices, R_{740}/R_{800}, R_{740}/R_{720}, and R_{440}/R_{690}, and the derivative fluorescence indexes, D_{705}/D_{722} and D_{730}/D_{706} were also all strongly correlated to the severity of wheat stripe rust. These indices are, therefore, suitable for use for monitoring the severity of wheat stripe rust based on the chlorophyll fluorescence reflectance extraction algorithm. Comparing the two chlorophyll fluorescence extraction algorithms it can be seen that the correlation between the chlorophyll fluorescence intensity estimated using the reflectance ratio index R_{440}/R_{690} and the severity of wheat stripe rust is the greatest, with a multiple correlation coefficient of 0.7187, while the correlation between the

chlorophyll fluorescence intensity extracted by the radiance method and the severity of wheat stripe rust is lower 0.6722. This is assumed to be due to the fact that the estimated chlorophyll fluorescence intensity based on the radiance method affects the accuracy of the estimates of fluorescence.

The resultant estimates and the verification of those results for the models constructed using the BP neural network and PLS algorithms showed that the R^2 of the models integrating both SIF and differential spectral indices as independent variables, between estimated DI and measured DI were more highly correlated than the models using only the differential spectral indices as independent variables. RMSE values were also lower for those models using only the differential spectral index as an independent variable. The results are consistent with those of jing xia[42] and Chen siyuan[43] et al. This is because the reflectance spectrum can be representative of the concentration of the biochemical components but cannot directly reveal the photosynthetic physiological state of the vegetation. Solar-induced chlorophyll fluorescence can sensitively reflect the vitality of the photosynthesis of the crop. Comprehensive utilization of the datasets can, nevertheless, provide canopy reflectance data for crop population growth and be used to identify chlorophyll fluorescence parameters sensitive to the vitality of the photosynthesis of crops. This can help improve the detection accuracy of the methods used to measure the severity of wheat stripe rust. In the selection of appropriate reflectance spectra, only the differential spectral index is used. The impact of using the vegetation index and absorption characteristic parameters remains to be investigated.

The accuracy of estimates of wheat stripe rust severity using remote sensing systems is not only related to the independent variables selected but is also affected by the modeling algorithm used. Choosing a suitable modeling method can improve the accuracy of the resultant estimates. In this paper, the PLS method, based on mathematical statistics; the machine-learning-based BP neural network method were applied to remote sensing data to test their abilities to detect the severity of wheat stripe rust. A cross-validation method was used to compare and analyze the accuracy of the estimates of disease severity of wheat stripe rust constructed by the two algorithms. The results showed that the BP neural network model provided better estimates than the PLS models. This is because the factors used by the PLS regression algorithm to establish the estimation model must be linearly independent, and so dimensionality reduction is required, which loses data information. Overall, it was clear that the BP neural network model should be the preferred method for estimating the severity of wheat stripe rust.

In this study, the SIF and differential spectral indices were used as independent variables to construct the models for estimating wheat stripe rust severity, but the relative contribution rates for the different parameters to each model's output were not considered. Future research could study how to determine the weight carried by each parameter in the process and apply this information to the development of improved models.

V. CONCLUSION

In order to improve the accuracy of the remote sensing detection of wheat stripe rust, this study made full use of the advantages of reflectance spectroscopy for the detection of crop biochemical parameters and the advantages of chlorophyll fluorescence in photosynthetic physiological diagnosis. During a set of research experiments evaluating the remote sensing detection of the severity of wheat stripe rust, a PLS and a BP neural network were tested. After comparing and analyzing the data, it was concluded that remote sensing detection of wheat stripe rust severity can both be realized using the differential spectral index alone or by using the differential spectral index and the solar-induced chlorophyll fluorescence in combination. However, the accuracy of the estimates made by the two models using the combination of data from the differential spectral index and the solar-induced chlorophyll fluorescence were all higher than that for the models constructed using the differential spectral index alone. By comparing the model algorithms, it was also seen that, if the differential spectral index and the canopy solar-induced chlorophyll fluorescence synergistic differential spectral index were used as sensitive factors, the coefficients of determination between the estimated DIs using the BP neural network model and the measured DIs was 0.955, which were greater than the coefficients produced when using the PLS model (0.916). Similarly, the RMSE were 0.068, which were smaller than the RMSE (0.091) using the PLS model.The model using the BP neural network algorithm was, therefore, better at estimating wheat stripe rust severity than the PLS model, and it is more suitable for the remote sensing detection of wheat stripe rust severity. These results have important significance for improving the accuracy of the real-world remote sensing detection of wheat stripe rust, and the analysis provides new ideas for further realizing large-area remote sensing monitoring of crop health.

ACKNOWLEDGMENTS

The authors gratefully acknowledge the financial support provided by the National Natural Science Foundation of China (41601467).

REFERENCES

[1] R. He, H. Li, and X. Qiao, "Using wavelet analysis of hyperspectral remote-sensing data to estimate canopy chlorophyll content of winter wheat under stripe rust stress," Int J Remote Sens. Vol. 39, 2018, pp.4059-4076.

[2] D. Liang, N. Liu, and D. Zhang, et al. "Discrimination of powdery mildew and yellow rust of winter wheat using high-resolution hyperspectra and imageries". Infrared and Laser Engineering. vol. 46, 2017, pp.138004_1-138004_9.

[3] Q. Zheng, W. Huang, and X. Cui, "New Spectral Index for Detecting Wheat Yellow Rust Using Sentinel-2 Multispectral Imagery". Sensors. vol.18, 2018, pp. 868-886

[4] J. Zhao , L. Huang , and W. Huang, "Hyperspectral measurements of severity of stripe rust

[5] on individual wheat leaves" . Eur J Plant Pathol , vol.139, 2014, pp.407–417.

[6] Y. Shi, W. Huang, and P. González-Moreno, "Wavelet-Based Rust Spectral Feature Set (WRSFs):A Novel Spectral Feature Set Based on ContinuousWavelet Transformation for Tracking ProgressiveHost-Pathogen Interaction of Yellow Rust on Wheat". Remote sensing, vol.525, 2018, pp. 1-19.

[7] Y. Shi, W. Huang, and X. Zhou. "Evaluation of wavelet spectral features in pathological detection and discriminationbof yellow rust and powdery mildew in winter with hyperspectral reflectance data". Journal of applied remote sensing. vol.11, 2017, pp.025-026.

[8] H. Wang, F. Qin, and L. Ruan, "Identification and Severity Determination of Wheat Stripe Rust and Wheat Leaf Rust Based on Hyperspectral Data Acquired Using a Black-Paper-Based Measuring Method". Plos one. vol.11, 2016, pp.1-25.

[9] L. Wang, J. Qu. "Satellite remote sensing applications for surface soil moisture monitoring: A review", Frontiers of Earth Science in China. vol.3, 2009, pp.237-247.

[10] J. E. McMurtrey, E. M. Middleton, and L. A. Corp, "Optical reflectance and fluorescence for detecting nitrogen needs in Zea mays L", IEEE International Geoscience& Remote Sensing Symposium. 2003, doi:10.1109/IGARSS.2003.1295594.

[11] D. Ashourloo, M. R. Mobasheri, and A. Huete. "Developing two spectral disease indices for detection of wheat leaf rust (Pucciniatriticina)". Remote Sensing. vol. 6, 2014, pp.4723-4740.

[12] W. K. Smith, J. A. Biederman, R. L. Scott, et al., "Chlorophyll Fluorescence Better Captures Seasonal and Interannual Gross Primary Productivity Dynamics Across Dryland Ecosystems of Southwestern North America," Geophys.Res.Lett. vol.45, 2015, pp.1-10.

[13] G. H. Krause and E. Weis, "Chlorophyll fluorescence and photosynthesis: the basics," Annu. Rev. Plant. Blog. Vol, 42, 1991, pp.313-349.

[14] N. Subhash, and V. Ravi, "Detection of mosaic virus disease in cassava plants by sunlight-induced fluorescence imaging: a pilot study for proximal sensing," Int.J.Remote. Sens. Vol. 36, 2015, pp.2880-2897.

[15] L. Liu, J. Zhao, and L. Guan, "Tracking photosynthetic injury of Paraquat-treated crop using chlorophyll fluorescence from hyperspectral data," Eur. J.Remote.Sens. vol.46, 2013, pp.459-473.

[16] D. Christen, S. Schönmann, and M. Jermini, "Characterization and early detection of grapevine (vitis vinifera) stress responses to esca disease by in situ chlorophyll fluorescence and comparison with drought stress," Environ.Exp.Bot. vol.60, 2007, pp.504-514.

[17] Y. Zhang et al., "Chlorophyll Fluorescence Sensing to Detect Stripe Rust in Wheat(Triticum aestivum L.)Fields Based on Fraunhofer Lines," Scientia Agricultura Sinica. 40(1), 78-83 (2007).

[18] Y. Zhang, W. Huang, and J. Wang, "Study on the severity of stripe rust in winter wheat using hyperspectral index," Trans. CSAE. vol.21, 2005, pp.97-103.

[19] J. Jiang, Y. Chen, and J.Zhang, "Using hyperspectral indices to diagnose severity of winter wheat stripe rust," Opt.Techol. vol.33, 2007, pp.620-623.

[20] Y. Xiong et al., "Estimation of forest leaf area index based on random forest model and remote sensing data," Transactions of the Chinese Society for Agricultural Machinery. 05(19), 159-166 (2017).

[21] L. Mo, "Prediction of wheat stripe rust using neural network," IEEE International conference on intelligent computing&intelligent systems. 2010, doi:10.1109/ICICISYS.2010.5658476.

[22] X. Hu, Z. Yang, and Z. Li, "Prediction of wheat stripe rust in hanzhong area by BP neural network," Acta Agriculturae Boreali-Occidentalis Sinica. vol.9, 2000, pp.28-31.

[23] GB/T 15795-2011, Rules for monitoring and forecast of the wheat stripe rust Puccinia striiformis West . GB/T 15795-2011.

[24] J. Luo, M. Huang, and J. Zhao, "Spectrum characteristics of winter wheat infected by aphid in filling stage," Trans. CSAE. vol.27, 2011, pp.215-219.

[25] J. Hu, L. Liu, and X. Liu, "Assessing uncertainties of sun-induced chlorophyll fluorescence retrieval using FluorMOD model," J.Remote.Sens. vol.19, 2015, pp.594-608.

[26] L. Liu, "Remote Sensing Principle and Application of Quantitative Vegetation", 1th ed, Science Press, 2014, pp. 146–153.

[27] K. Plascyk, and F. Gabriel, "The Fraunhofer line discriminator MKII-an airborne instrument for precise and standardized ecological luminescence measurement," IEEE.T.Instrum.Meas. vol. 24, 1975, pp.306-313.

[28] S. Maier, K. Günther, and M. Stellmes, "Sun-induced fluorescence: A new tools for precision farming". 2003, pp.209-222.

[29] X. Liu, "Study of sun-induced cholorophy retrieval using remote sesing methods," Ed., 2016, pp. 17-19, University of Chinese Academy of Sciences, Beijing, China.

[30] X. Liu, and L. Liu, "Improving Chlorophyll Fluorescence Retrieval Using Reflectance Reconstruction Based on Principal Components Analysis," IEEE Geosci. Remote. S. vol.12, 2015, pp.1645-1649.

[31] R. Pu, and P. Gong, "Hyperspectral remote Sensing and applications", 1th ed., 2003, pp.53, higher Education Press.

[32] J. Jiang, Y. Chen, and W. Huang, "Estimation of canopy chlorophyll density of wheat under stripe rust stress by using hyperspectral differential index," Spectrosc.Spect.Anal. vol.30, 2010, pp.2243-2247.

[33] J. Yue, H. Feng, G. Yang, "A Comparison of Regression Techniques for Estimation of Above-Ground Winter Wheat Biomass Using Near-Surface Spectroscopy," Remote.Sens. vol.10, 2018, pp.66.

[34] L. Liu, Y. Zhang, and J. Wang, "Detecting Photosynthesis Fluorescence under Natural Sunlight Based on Fraunhofer Line," J. Remote.Sens. vol.10, 2006, pp.130-137.

[35] L. Liu. Y. Zhang, and J. Wang, "Detecting solar-induced chlorophyll fluorescence from field radiance spectra based on the Fraunhofer line principle," IEEE.T. Geosci.Remote. vol.43, 2005, pp.827-832

[36] P. Zarco-Tejada, J. Miller, and G. Mohammed, "Chorophyll fluorescence effects on vegetation apparent reflectance: I. Leaf-level measurements and model simulation," Remote.Sens.Environ. vol.74, 2000, pp.582-595.

[37] P. Zarco-Tejada, J. Miller, and G. Mohammed, "Chlorophyll fluorescence effects on vegetation apparent reflectance: II.laboratory and airborne canopy-level measurements with hyperspectral data," Remote.Sens.Environ. vol.74, 2000, pp.596-608.

[38] S. Dobrowski, J. Pushnik, and P. Zarco-Tejada, "Simple reflectance indices track heat and water stress induced changes in steady state chlorophyll fluorescence", Remote.Sens.Enviro. vol.97, 2005, pp.403-414.

[39] P. Zorco-Tejada, J. Pushnik, S. Dobrowski, "Steady-state chlorophll a fluorescence detection from canopy derivative reflectance and double-peak red-edge effects," Remote.Sens.Enviro. vol.84, 2003, pp.283-294.

[40] N. Broge, and E. Leblanc, "Comparing prediction power and stability of broadband and hyperspectral vegetation indices for estimation of green leaf area index and canopy chlorophyll density," Remote.Sens.Enviro. vol.76, 2003, pp.156-172.

[41] D. Haboudane, J. Miller, and E. Pattey, "Hyperspectral vegetation indices and novel algorithms for predicting green LAI of crop canopies: Modeling and validation in the context of precision agriculture," Remote.Sens.Enviro. vol.90, 2004, pp.337-352.

[42] X. Jing, Z. Bai, "Wheat stripe rust monitoring by random forest algorithm combined with SIF and reflectance spectrum "Transactions of the Chinese Society of Agricultural Engineering. vol.35, 2019, pp.154 − 161.

[43] S.Chen , X.Jing. "Detection of wheat strip rust using solar-induced chlorophyll fluorescence spectral indices," Remote sensing technology and application. Vol.34, 2019, pp.511-520.